

42

43 **Highlights**

44

- 45 • Long photoperiods increase the photosynthetic activity of certain subarctic
- 46 macrophytes
- 47 • Increased CO₂ had no effect on tested macrophytes
- 48 • Highest increases of photosynthetic activity of *Ascophyllum nodosum* and *Zostera*
- 49 *marina* at long day lengths; smaller increase for *Fucus vesiculosus*
- 50 • Subarctic macrophytes, expanding as sea ice retreats, will benefit from long
- 51 summer days

52

53

54 **Keywords**

55

56 Macrophytes; subarctic; electron transport rate; continuous photoperiod and carbon

57 dioxide.

58

59

60 **1 Introduction**

61

62 The presence of macroalgae assemblages in the Arctic is often limited by extended

63 sea-ice cover that reduces submarine light penetration (Krause-Jensen et al., 2012;

64 Krause-Jensen and Duarte, 2014; Wulff et al., 2009). However, an Arctic largely free of

65 sea ice in summer, as predicted by the year 2037 (IPCC Panel, 2014; Wang and Overland,

66 2009), may favour the entrance of new species into the Arctic and the expansion of

67 existing Arctic vegetation (Krause-Jensen and Duarte, 2014). Indeed, the northward

68 extension range of macroalgae, mainly Phaeophyta, but also Chlorophyta and

69 Rhodophyta has been observed around 78 °N in Svalbard (Fredriksen et al., 2014). An

70 increase of macrophyte biomass has also been detected together with the upward

71 movement of sublittoral algal species to the littoral zone and a biodiversity increase in

72 this Arctic region, likely related to climate warming (Weslawski et al., 2010). Arctic

73 warming has already led to the reappearance of the blue mussel, *Mytilus edulis*, in

74 Svalbard after 1,000 year absence (Berge et al., 2005) as well as an increase of the Arctic

75 cod fishery due to the poleward expansion of cod habitat (Kjesbu et al., 2014). At a global

76 scale, 75 % of the range shifts studied in marine species, including macrophytes and

77 phytoplankton among other taxa, are in poleward direction due to climate warming (Sorte

78 et al., 2010).

79 Atmospheric carbon dioxide concentration has increased ~40% since the beginning of

80 the industrial era (Zeebe, 2012), currently exceeding 400 ppm. Yet, *p*CO₂ in the Arctic

81 Ocean ranks amongst the lowest values reported across the open ocean (Takahashi et al.,

82 2009), presenting characteristically low *p*CO₂ (< 200 μatm) due to intense spring

83 phytoplankton blooms (Bates et al., 2006; Fransson et al., 2009; Holding et al., 2015) and

84 the influence of sea ice melting during summer (Rysgaard et al., 2009).

85 Marine macrophyte communities tend to be autotrophic, where photosynthesis
86 dominates over respiration (Duarte and Cebrián, 1996), thereby leading to a depletion of
87 CO₂, potentially reaching limiting *p*CO₂ levels (Krause-Jensen et al., 2016; Mercado and
88 Gordillo, 2011). In parallel, atmospheric CO₂ is predicted to increase, reaching 1000 ppm
89 before the end of the century under some scenarios (IPCC Panel, 2014). Such levels may
90 further stimulate submerged sub-arctic vegetation (Krause-Jensen and Duarte, 2014).

91 Most habitat-forming macroalgae in the Arctic are originally from North Atlantic and
92 North Pacific regions (Wilce and Dunton, 2014; Wulff et al., 2009). *Zostera marina* has
93 been reported in the Arctic up to 70°N, although its presence is scarce (reviewed by
94 Olesen et al., 2015). Intertidal belts of the macroalgae *Ascophyllum nodosum* are present
95 up to 69.7° N (reviewed by Marbà et al., 2017) and *Fucus vesiculosus* has been found as
96 far north of 75 °N as the Svalbard Archipelago (Florczyk and Latala, 1989; Hansen and
97 Haugen, 1989).

98 Warming and consequently retreating sea-ice is increasing the available habitat,
99 leading to a forecasted expansion of subarctic and Arctic vegetation into the Arctic Ocean
100 that would increasingly expose the vegetation to the extended daylight period of the
101 Arctic summer (Krause-Jensen et al., 2016; Krause-Jensen and Duarte, 2014). Potentially,
102 continuous daylight increases the hours of C-fixation through photosynthesis, increasing
103 its primary productivity. However, the excess of light energy and long photoperiods
104 might induce photoinhibition damage and prevent growth (Velez Ramirez et al., 2011).
105 Therefore, studying the physiology and the photosynthetic machinery of subarctic marine
106 macrophytes under a continuous photoperiod, characteristic of the Arctic summer, is key
107 to evaluate the probabilities of a forecasted poleward expansion. Research on the effect
108 of continuous light on photosynthetic organisms is scarce and has mainly been related to
109 use in greenhouse food production (Velez Ramirez et al., 2011).

110 The physiological responses of a canopy-forming species to different levels of light
111 intensity, CO₂ and temperature has been evaluated in the Antarctica (Iñiguez et al., 2017).
112 In the same region, the transition from late winter to summer on phytoplankton
113 physiology has been evaluated focussing on variable light intensities (McMinn et al.,
114 2010) in combination with increased CO₂ (Hoppe et al., 2015). In the Arctic Ocean, the
115 effect of increased CO₂ has been physiologically tested in macroalgae (Iñiguez et al.,
116 2016) and phytoplankton in combination with light intensity and temperature (Hoppe et
117 al., 2018, 2017). The physiological responses of polar macro and microphytes to
118 continuous photoperiod remains insufficiently explored. Krause-Jensen et al. (2016)
119 concluded that day lengths longer than 21 hours, characteristic of Arctic summers, were
120 conducive to sustain a high pH in seawater as a result of photosynthesis by macro-
121 autotrophs. They also concluded that experimental increase in CO₂ concentration
122 stimulated the capacity of macrophytes to deplete CO₂. However, they analysed an
123 assemblage of three species (*Z. marina*, *A. nodosum* and *F. vesiculosus*) and did not
124 explore the species-specific response of photosynthetic physiology to longer
125 photoperiods and increased CO₂, neither the interactive effect between the day length and
126 enhanced CO₂, which are the aims of our study.

127 Marine macrophytes are often limited by CO₂ because the boundary layers formed
128 around the blades limit the entrance of CO₂ by diffusion due to its thickness (Hendriks et

129 al., 2017), which together with high primary productivity rates in densely vegetated areas
130 result in low CO₂ levels close to the blade surface (Bowes and Salvuci, 1989; Holbrook
131 et al., 1987; Hurd et al., 2009). The low CO₂ concentration characteristic of Arctic and
132 subarctic waters due to strong biological uptake in spring and melting sea ice in summer
133 (Bates et al., 2006; Fransson et al., 2009; Meire et al., 2015; Takahashi et al., 2009) may
134 cause CO₂ limitation, - with the risk being particularly likely in vegetated coastal habitats
135 that represent hot spots of productivity and CO₂-draw down. Productivity of subarctic
136 macrophytes could, hence, be limited by CO₂ similar to the limitation of phytoplankton
137 productivity in the Arctic (Engel et al., 2014; Hein and Sand-Jensen, 1997; Holding et al.,
138 2015).

139 Key to understanding how marine vegetation will respond to predicted increased levels
140 of dissolved inorganic carbon (DIC) and longer photoperiods is their species-specific
141 photosynthetic physiology (Koch et al., 2013). The majority of autotrophs have a higher
142 photosynthetic affinity for CO₂ than bicarbonate (HCO₃⁻) (Bowes, 1985; Madsen and
143 Sand-Jensen, 1991). In the oceans, an increase in CO₂ concentration will increase the total
144 DIC and hydrogen ion concentration (H⁺) leading to a decrease in pH and a change in the
145 carbon species. The increase in CO₂ availability will probably enhance photosynthesis
146 and growth of seagrasses and many macroalgae as well as the competition between
147 species and would benefit those with a greater ability to rapidly sequester CO₂ (Koch et
148 al., 2013).

149 The majority of marine macroalgae and seagrass are supposed to possess Rubiscos that
150 are not saturated at the current ocean DIC concentration, thus these organisms have
151 Carbon Concentrating Mechanisms (CCMs), which finally increase CO₂ around Rubisco
152 relative to the CO₂ concentration in seawater, through an active transport of CO₂ and/or
153 HCO₃⁻ inside the cell (Giordano et al., 2005). Despite the widespread presence of CCMs,
154 different species-specific responses to increased levels of CO₂ has been observed (Beer
155 et al., 2014; Beer and Rehnberg, 1997; Sand-Jensen and Gordon, 1984; Koch et al., 2013;
156 Surif and Raven, 1989). Many marine macrophytes possess the capacity to utilize HCO₃⁻
157 for photosynthesis (Giordano and Maberly, 1989; Koch et al., 2013; Mercado et al., 2009;
158 Surif and Raven, 1989), although it does not indicate that their photosynthesis might be
159 saturated at present CO₂ conditions. In fact, all analysed seagrass and most brown
160 macroalgae showed that an increase in DIC concentrations promotes higher
161 photosynthetic and growth rates (Koch et al., 2013). In conditions of severe CO₂
162 limitation, the high availability of HCO₃⁻ increases C acquisition, but it is energetically
163 expensive and CO₂ remains preferable for photosynthesis as compared to HCO₃⁻ due to
164 lower photosynthetic K_{0.5} values for CO₂ than for HCO₃⁻ in seagrasses and macroalgae
165 (Sand-Jensen and Gordon, 1984).

166 The brown macroalgae *F. vesiculosus* is an exception, with photosynthetic rates being
167 saturated at current DIC levels (Koch et al., 2013; Raven and Osmond, 1992) and has a
168 high affinity and capacity for DIC uptake by non-diffusive mechanisms (Mercado et al.,
169 2009). Conversely, photosynthesis of *A. nodosum* is not CO₂-saturated, even though its
170 capacity for HCO₃⁻-use has been demonstrated (Koch et al., 2013; Surif and Raven, 1989).
171 The utilization of HCO₃⁻ in seagrasses is generally less efficient than in macroalgae (Beer
172 et al., 2014; Beer and Rehnberg, 1997; Sand-Jensen and Gordon, 1984) although for *Z.*

173 *marina* it is not confirmed whether photosynthesis is saturated at current CO₂ levels
174 (Koch et al., 2013). *A. nodosum*, *F. vesiculosus* and *Z. marina* therefore represent 3 test
175 organisms for which different responses to increased CO₂ could be expected.

176 Polar macroalgae are generally hypothesized to have a competitive advantage in a
177 future high CO₂ environment (Raven et al., 2002a, 2002b). In cold regions the entry of
178 CO₂ by diffusion into the cell seems to be more widespread for brown and red
179 macroalgae, than the same species of macroalgae in temperate regions, avoiding the need
180 of CCMs and making them more prone to stimulation by increased CO₂ than temperate
181 macroalgae (Mercado and Gordillo, 2011; Raven et al., 2002a, 2002b), although higher
182 CO₂ dependence has been attributed to red polar macroalgae (Raven et al., 2002b).

183 Here we experimentally test the hypothesis that increased CO₂ supply (400 and 1000
184 ppm) relative to the low ambient CO₂ levels of Arctic waters (200 ppm) increase
185 photosynthesis of subarctic marine macrophytes. Such an increase would support the
186 projected expansion of marine vegetation in the future high Arctic given that
187 photosynthetic activity of individual leaves is related with estimates of macrophyte
188 productivity at a community-level (Silva et al., 2005). We also evaluate the effect of
189 longer photoperiods (12:12, 15:09, 18:06, 21:03 and 24:00 light:dark hours) on
190 photosynthetic activity to assess whether long days/continuous daylight, as resulting from
191 longer open water periods in the future Arctic, hamper or stimulate photosynthesis. We
192 use two macroalgae species (*A. nodosum* and *F. vesiculosus*) and one seagrass species (*Z.*
193 *marina*) as test organisms.

194 195 **2 Materials and methods**

196 197 2.1. Experimental set-up and sampling

198
199 Brown macroalgae (*A. nodosum*, *F. vesiculosus*) fronds were collected in the lower
200 intertidal zone and seagrass (*Z. marina*) shoots, sparse in this region (Olesen et al., 2015),
201 were collected from shallow waters (1 to 3 m depth) at the central part of Kobbefjord
202 (64°10'N and 51°29'W, Godthåbsfjord, Greenland) in early June 2014.

203 They were kept cool and humid during the 30 h transport by airplane to the laboratories
204 of the Mediterranean Institute for Advanced Studies (IMEDEA, Mallorca, Spain). In the
205 laboratory facilities they were acclimated in artificial seawater to the photoperiod to
206 which they were exposed at collection (21:03h, light:dark hours, in the Godthåbsfjord in
207 early June), during 10 days in a climate controlled room at 4 °C.

208 After the acclimation period, undamaged tips of *A. nodosum* and *F. vesiculosus* and
209 shoots of *Z. marina* were transferred into nine aquaria (6 L), with controlled photoperiod,
210 temperature and *p*CO₂ levels. The total biomass of macrophytes in each aquarium was
211 2.7-3.7 g dry weight (DW), yielding a biomass density of 0.45-0.61 g DW L⁻¹, mimicking
212 dense vegetation. The aquaria were exposed to three *p*CO₂ levels (200, 400 and 1000 ppm
213 in the absence of macrophytes) with three replicated aquaria per level. 200 ppm reflected
214 contemporary *p*CO₂ levels in subarctic surface waters in spring/summer in
215 Godthåbsfjord, close to Kobbefjord (Meire et al., 2015). The highest *p*CO₂ manipulation
216 (1000 ppm) was set to the predicted scenario of atmospheric *p*CO₂ by 2100 (IPCC Panel,

217 2014), and 400 ppm represented an intermediate level (Fig. 1). To mimic the
218 photosynthetic active radiation (PAR) within *in situ* canopies, the aquaria were
219 illuminated with $111 \pm 5 \mu\text{mol photons m}^{-2} \text{s}^{-1}$ of PAR at the water surface using 2 lamps
220 with 54 W fluorescent tubes. This light level was about half of the maximum PAR
221 reported in Greenland fjords close to the Godthåbsfjord (204-289 $\mu\text{mol photons m}^{-2} \text{s}^{-1}$)
222 at 2m depth during May and June 2013 (Olesen et al., 2015). This experiment also
223 provided the results described in Krause-Jensen et al. (2016).

224 The aquaria were filled with artificial seawater made from distilled water, Reef
225 Crystals® and NaCl to obtain a similar salinity (30.2 ± 0.42 , subarctic range: 28.9-31.7)
226 and alkalinity ($2241 \mu\text{mol kg SW}^{-1} \pm 31.3$, measured in the sampled area: 1980-2240 μmol
227 kg SW^{-1}) as conditions in the field. The artificial seawater was pre-exposed to UV to limit
228 the growth of microorganisms during the experiment. To reach targeted $p\text{CO}_2$ levels, air
229 was circulated through soda lime tubes to remove the CO_2 present and it was mixed with
230 pure CO_2 gas in a bottle with marbles to maximize the mixing surface area. The
231 concentration of air and pure CO_2 in the mixing bottle was regulated with mass flow
232 controllers (MFCs, AALBORG GFC-17, US). The targeted $p\text{CO}_2$ concentration was
233 continuously supplied to the aquaria through porous bubble curtains. pH was measured
234 *in continuum* with pH electrodes (Omega, PHE-1411) and recorded at 15 min intervals
235 (IKS Aquastar, Germany; for more details see Krause-Jensen et al., 2016). When seawater
236 in the aquaria had reached a stabilized pH and targeted $p\text{CO}_2$ was reached, the same
237 number of tips of *A. nodosum* and *F. vesiculosus* and shoots of *Z. marina* (6 individuals
238 of each species) were attached to the base of the aquaria, with every individual identified
239 with a label. The macrophytes in each of the six aquaria were cycled through a series of
240 random photoperiods (12:12h, 15:9h, 18:6h, 21:3h and 24:0h, light:dark hours), that were
241 run as a whole experimental unit and maintained 3 days at each photoperiod treatment
242 (Fig. 1). Total alkalinity (TA) was measured at the start and end of each photoperiod and
243 interpolated linearly over the 3-days period. Sampled seawater was poisoned with 0.02
244 ml of a saturated solution of HgCl_2 (Merck, Analar) in order to avoid biological alteration
245 of the sample during storage. TA was determined with a Titrand 808 (Metrohm) by open
246 cell titration as described in Dickson et al., (2007). Certified CO_2 seawater reference
247 material (CRM Batch136) from the Andrew Dickson lab at UC San Diego was used to
248 warrant the accuracy of results. TA and pH_{NBS} were used to calculate the CO_2
249 concentrations using CO2SYS Pierrot et al., (2006), with dissociation constants from
250 Mehrbach et al., (1973) refitted by Dickson and Millero, (1987) and HSO_4^- using
251 Dickson, (1990). In between photoperiod treatments, seawater was changed and replaced
252 by seawater pre-treated with CO_2 gas at the targeted $p\text{CO}_2$ levels.

253 The photosynthetic capacity of the three macrophyte species was measured through
254 photosynthesis-irradiance curves (PI curves), also known as rapid light curves (RLC),
255 showing the response of the chlorophyll *a* fluorescence to a range of light intensities
256 (Falkowski and Raven, 2013; Ralph and Gademann, 2005). The measurements were done
257 after 3 days exposure to an experimental photoperiod on two of the six individuals of each
258 species present in two out of three replicated aquaria using Pulse Amplitude Modulation,
259 with a diving-PAM fluorometer (Walz, Germany). The measurements were always done
260 on the same individuals. *Z. marina* measurements were conducted on the second youngest

261 leaf and 4 cm above the meristem. On *A. nodosum* and *F. vesiculosus* measurements were
 262 done below the youngest bladder.

263 To avoid excessive manipulation of macrophytes, the measurements were done inside
 264 the aquaria. Using a PAM leaf-clip, the tissue, was dark-adapted for 5 min as done in
 265 previous studies (e. g. Anton et al., 2018; Apostolaki et al., 2014; Hendriks et al., 2017)
 266 and was illuminated with a series of nine increasing actinic light intensities (from 0 to
 267 maximum 616 $\mu\text{mol PAR m}^{-2} \text{s}^{-1}$) at intervals of 10s to produce a RLC. The maximum
 268 relative electron transport rate ($rETR_{\text{max}}$, $n = 12$ per species and per photoperiod) was
 269 calculated by fitting the RLC data with the non-linear model (Harrison and Platt, 1986;
 270 Platt et al., 1982; Ralph and Gademann, 2005):

$$271 \quad rETR = rETR_{\text{max}} \times (1 - e^{(-\alpha \times PAR_{\text{incident}} / rETR_{\text{max}})}) \quad (\text{Eq. 1})$$

272
 273 The photosynthetic parameters $rETR_{\text{max}}$, photosynthetic or quantum efficiency (α) and
 274 saturating irradiance (I_k , $I_k = rETR_{\text{max}} / \alpha$) were estimated by fitting the data of the RLC
 275 to Eq. 1 using R version 1.0.44 (R Core Team, 2014). Even though *A. nodosum* and *Z.*
 276 *marina* showed no asymptotic approximation to the $rETR_{\text{max}}$ in some cases due to the
 277 limited range of actinic light intensities above light saturation (Fig. A1 and A3), $rETR_{\text{max}}$
 278 could still be estimated from the curvature of the RLC.
 279

280 281 2.2. Statistical analysis

282
 283 We evaluated if CO_2 (3 levels) and photoperiod (5 levels) had an effect on
 284 photosynthetic responses, as represented by $rETR_{\text{max}}$, α and I_k , and if such effects were
 285 similar or different for the three macrophyte species tested. The experiment was a split-
 286 plot design due to restricted randomization for photoperiod, i.e. each level of photoperiod
 287 was run separately (whole plot) and without replication. Experimental units (whole plots)
 288 consisted of six aquaria that were grouped into 3 levels of CO_2 with 2 replicates for each
 289 CO_2 treatment at each photoperiod (Fig. 1). The experimental units were sub-divided or
 290 split into different periods (sub-plots) to test the effects of varying photoperiod. However,
 291 aquaria were nested within CO_2 treatment, as the same CO_2 treatment was applied to the
 292 same aquarium for all photoperiods. All three species were randomly sampled for each
 293 sub-plot and, consequently, species variation was a factor fully crossed with the two
 294 treatment factors. Finally, individual macrophyte specimens within each aquarium were
 295 not replaced between different photoperiod levels and constituted a random factor nested
 296 within CO_2 treatment and aquarium. The following split-plot model (using capital letters
 297 for random factors in Eq. 2) was employed for the three photosynthesis variables
 298 separately ($rETR_{\text{max}}$ and I_k were log-transformed):
 299

$$300 \quad Y_{ijkl} = \mu + \underbrace{c_i + A_l(c_j) + I_m(A_l(c_j))}_{\text{whole-plot}} + \underbrace{p_j + p_j \times c_i + P_j \times A_l(c_j) + P_j \times I_m(A_l(c_j))}_{\text{split-plot}}$$

$$301 \quad + \underbrace{s_k + s_k \times c_i + s_k \times p_j + s_k \times p_j \times c_i}_{\text{species variations fixed effects}}$$

(Eq. 2)

where μ is the overall mean, c_j = CO₂ treatment, p_i = photoperiod, s_k =species, A_l = aquarium and I_m = individual macrophyte specimen. The three main effects (p_i , c_j , and s_k) and their interaction were fixed effects, whereas variation among aquaria (A_l) and macrophyte individuals (I_m) and interactions derived from these were random. Marginal means were calculated for all the fixed effects and back-transformed to the geometric mean for the two log-transformed response variables.

The split-plot model is a mixed linear model and was analysed using PROC MIXED in SAS version 9.3. Statistical testing for fixed effects (F-test with Satterthwaite approximation for denominator degrees of freedom) and random effects (Wald Z-test) were carried out at a 5% significance level. The F-test for fixed effects was partial, i.e. considering the specific contribution of the given effect in addition to all other factors.

3 Results

The RLCs (Fig. A1, A2, A3) typically flattened out for all three species around 200 $\mu\text{mol photons m}^{-2} \text{ s}^{-1}$, but light saturation (I_k) was reached at lower light levels for *F. vesiculosus* and *Z. marina* than *A. nodosum*. Photoinhibition, lowering of photosynthetic rates at higher irradiances, was not detected.

$r\text{ETR}_{\text{max}}$ and saturating irradiance (I_k) were significantly different between photoperiods with values increasing progressively up to the 24h-light photoperiod (Table 1). The largest differences in $r\text{ETR}_{\text{max}}$ were found between the 21 h and 24 h photoperiod with increases from 20.4 up to 30 $\mu\text{mol electrons m}^{-2} \text{ s}^{-1}$, when all species data was pooled. At the photoperiods of 12 h, 15 h and 18 h the $r\text{ETR}_{\text{max}}$ was variable (21.8, 23.5 and 23.5 $\mu\text{mol electrons m}^{-2} \text{ s}^{-1}$, respectively when all species data were pooled).

The highest average values of $r\text{ETR}_{\text{max}}$ and I_k were found for *A. nodosum* (Fig. 2a, c, Table 1). $r\text{ETR}_{\text{max}}$ increased 15%, on average, from 200 ppm of $p\text{CO}_2$ to 1000 ppm (from 21.2 to 24.4 $\mu\text{mol electrons m}^{-2} \text{ s}^{-1}$) although the effect of the CO₂ treatment was not significant (Table 1). The photosynthetic efficiency, α , was significantly different between species with higher values for both macroalgae compared to *Z. marina* (Fig. 2b, Table 1). The CO₂ effect on α was not significant but a gradual increase of 10% was observed from 200 to 1000 ppm (Table 1), while I_k did not show an effect of CO₂ (Table 1). The interaction effect between the different photoperiods and the species was significant for α and I_k , but not for $r\text{ETR}_{\text{max}}$ (Fig. 3, Table 1). *Z. marina* showed the highest increase in $r\text{ETR}_{\text{max}}$ on average from the photoperiod of 12 h to 24 h (10.7 $\mu\text{mol electrons m}^{-2} \text{ s}^{-1}$); followed by *A. nodosum* (9.9 $\mu\text{mol electrons m}^{-2} \text{ s}^{-1}$) and the lowest increase was observed in *F. vesiculosus* (3.2 $\mu\text{mol electrons m}^{-2} \text{ s}^{-1}$, Fig. 3a).

The interaction effect between CO₂ treatments and species was not significant for any of the photosynthetic responses, but *A. nodosum* showed the highest $r\text{ETR}_{\text{max}}$ and I_k at 1000 ppm (Fig. 4). The three photosynthetic parameters ($r\text{ETR}_{\text{max}}$, α and I_k) showed significant residual variation only while other random effects were not significant, which

346 indicates that variations associated with using different aquarium and analysis on
347 individual macrophyte specimen were relatively small compared to variations associated
348 with the photosynthetic activity.

349
350

351 **4 Discussion**

352

353 Our results showed a significant increase in photosynthetic capacity in response to
354 longer photoperiod, since $rETR_{max}$ increased from 21 h to 24 h for the three species tested
355 after 3 days of incubation. During shorter photoperiods (12 h to 18 h) $rETR_{max}$ was
356 variable and lower than at 24 h for the three species tested. The CO_2 -effect tended to be
357 positive but non-significant. Our results showed maximum $rETR_{max}$ at continuous
358 daylight for all three species, indicating an increase of their photosynthetic capacity. The
359 responses were variable among species: *Z. marina* and *A. nodosum* showed the highest
360 increases in $rETR_{max}$ with increasing daylight hours whereas the increase of *F.*
361 *vesiculosus* was smaller. The photosynthetic efficiency, α , in both macroalgae was similar
362 and higher than in *Z. marina* up until the photoperiod of 21 h was reached. At continuous
363 light, α showed variations both in *A. nodosum* and *F. vesiculosus*.

364 Along with the increase of its photosynthetic capacity at continuous daylight, our
365 results indicated no stress, as Yield (Fv/Fm) in 24 h light for *A. nodosum*, *F. vesiculosus*,
366 nor *Z. marina* was no different from other photoperiods and showed no decreasing trend
367 over time. These results indicate that the three studied macrophytes species could
368 potentially benefit from increased day length, at least on short time scales (as interfered
369 from 3 days of incubation), however *Z. marina* might encounter more difficulties than
370 macroalgae as they expand northward. Indeed, the presence of *Z. marina* in the subarctic
371 is scarce while the two macroalgae form intertidal subarctic belts. Our results for *A.*
372 *nodosum* agree with those of Strömngren, (1978), using specimen from the North Sea and
373 Norwegian Sea where *A. nodosum*, *Fucus serratus* and *Pelvetia canaliculate* increased
374 its growth up to 24 h whereas *F. vesiculosus* only increased up to 20 h of daylight. The
375 small increase in $rETR_{max}$ of *F. vesiculosus* compared with the increase of *A. nodosum*
376 and *Z. marina* at continuous daylight could explain their current presence in the high-
377 Arctic (Florczyk and Latala, 1989; Hansen and Haugen, 1989). Other species such as
378 *Ulva lactuca* and *Porphyra umbilicalis* from the North Sea did not increase their growth
379 at photoperiods greater than 16 h (Fortes and Lüning, 1980). Reduced photosynthetic
380 rates from 21 to 24 h daylight in species from the North Sea and Norwegian Sea are likely
381 caused by high photon flux rates leading to photoinhibition, light-induced reduction in
382 the photosynthetic capacity of the macrophytes, to protect the photosynthetic apparatus,
383 suggesting that macrophytes from different latitudes might regulate their photosynthetic
384 rates differently. Moreover, the Antarctic brown alga (*Adenocystis utricularis*) showed
385 faster photoinhibition than brown macroalgae of temperate zones (Hanelt, 1996).
386 Photoinhibition might be produced by continuous high irradiances, low temperatures and
387 CO_2 limitation (Beer et al., 2014). Before photoinhibition occurs, there are defence
388 mechanisms that down-regulate photosynthesis to dissipate the excess light energy such
389 as the xanthophyll cycle, the Mehler reaction or the use of Carbon Concentration

390 Mechanisms (CCMs). Under conditions of CO₂-limitation and excess light energy, the
391 Mehler reaction diverts the excess of electrons towards the production of H₂O₂ and
392 ultimately water. However, the Mehler reaction cannot be detected by PAM fluorometry
393 (Beer et al., 2014). CO₂-limitation and excess light energy also might lead into the use of
394 CCMs, increasing CO₂ concentration inside the cell and raising the use of energy. In our
395 study, CO₂ concentration was not limiting, and neither were light or temperature. We
396 chose to use PAM fluorometry, despite its shortcomings of only assessing part of the
397 photosynthetic response, because it is a non-invasive technique that does not overly stress
398 or damage the macrophyte, which is crucial in experiments with repeated measures over
399 some period of time.

400 rETR_{max} and Ik of *A. nodosum* and *Z. marina* increased slightly, yet insignificantly, in
401 response to increasing CO₂, while *F. vesiculosus* did not show any response. Other studies
402 show that the arctic macroalgae *Alaria esculenta* was positively affected by increased
403 CO₂, showing an increase of rETR_{max}, α and Ik along with increasing growth rates, while
404 the species *Desmarestia aculeata* responded by decreasing rETR_{max} and growth rates
405 (Iñiguez et al., 2016). The small response of *A. nodosum* agrees with the notion that this
406 macroalgae is not CO₂-saturated at ambient levels and diffusive entry of CO₂ seemed to
407 be required (Koch et al., 2013; Surif and Raven, 1989), while the absence of response of
408 *F. vesiculosus* might indicate that it is CO₂-saturated at ambient levels (Koch et al., 2013;
409 Raven and Osmond, 1992) and had high capacity for DIC uptake by non-diffusive
410 mechanisms (Mercado et al., 2009). Increased CO₂ might benefit subarctic *A. nodosum*
411 because it is not currently CO₂-saturated and the diffusive entry of CO₂ or CCMs based
412 on HCO₃⁻ usage are required (Johnston and Raven, 1986; Koch et al., 2013; Surif and
413 Raven, 1989), while *F. vesiculosus* was not affected by increased CO₂ probably due to its
414 currently CO₂-saturated stage and its capacity for non-diffusive mechanisms (Koch et al.,
415 2013; Raven and Osmond, 1992). The seagrass *Z. marina* can be either CO₂-saturated or
416 -limited at ambient levels (Koch et al., 2013). We observed a positive response, though
417 non-significant of *Z. marina* to increased CO₂, in line with CO₂-stimulation of seagrass
418 photosynthesis observed in other regions (Koch et al., 2013).

419 Our results show a non-significant interaction between increased CO₂ concentration
420 and increased photoperiods. CO₂-limiting environments generally increase the use of
421 CCMs, producing photoinhibition and decreasing the photosynthetic activity and growth.
422 Excess of light irradiance also might produce photoinhibition and a decrease of
423 photosynthetic activity. Our results indicate that continuous daylight at their natural
424 submerged irradiance ($111 \pm 5 \mu\text{mol photons m}^{-2} \text{s}^{-1}$ of PAR) lead to a positive
425 photosynthetic response of the three species tested while no significant response was
426 observed to increased CO₂.

427
428

429 **5 Conclusions**

430 Our results suggest that a continuous photoperiod, characteristic of Arctic summers,
431 may benefit the subarctic macrophytes tested in this study, increasing their photosynthetic
432 activity. *A. nodosum*, *F. vesiculosus* and *Z. marina*, hence, take advantage of increased
433 daylength during the Arctic summer as they migrate poleward with decreasing ice cover.

434 As they expand northward, they will probably be able to successfully cope with 24 h of
435 darkness during the Arctic winter since they are already present at 69.7° N (*A. nodosum*,
436 reviewed by Marbà et al., 2017), 75° N (*F. vesiculosus*, Florczyk and Latala, 1989;
437 Hansen and Haugen, 1989) and 70° N (*Z. marina*, reviewed by Olesen et al., 2015), and
438 thus exposed to photoperiods of long daylight and darkness. Nevertheless, further
439 research is needed on the interactive effects of day length and increased CO₂ with
440 nutrients availability, salinity and light intensities on photosynthesis of arctic and
441 subarctic macrophyte. Melting ice and coastal erosion leads to reduced light penetration
442 due to increased turbidity altering how macrophytes are distributed (Traiger and Konar,
443 2018) and been negatively affected (Bonsell and Dunton, 2018; Filbee-Dexter et al.,
444 2019). Freshwater accumulation is reducing nutrient inventories in the arctic water
445 column (Coupel et al., 2015; Yun et al., 2016) probably due to strong stratification
446 (McLaughlin and Carmack, 2010; Post et al., 2013). Gordillo *et al.*, (2006) showed a high
447 resilience to nutrient-limitation of many arctic macrophytes. Our results demonstrate that
448 continuous photoperiod stimulates the photosynthesis of the subarctic macrophytes tested
449 and support the forecasted poleward expansion of subarctic vegetation into the high-
450 Arctic (Krause-Jensen and Duarte, 2014). However, the spread of existing Arctic
451 macroalgae with climate change needs to be further studied focussing on the interactive
452 effects of long day length with CO₂, nutrients availability, salinity and light intensities.

453

454

455 **6 Acknowledgments**

456 This research was funded by the Danish Environmental Protection Agency within the
457 Danish Cooperation for Environment in the Arctic program. We thank J. Thyrring for his
458 help on the field, J. Baldrich and E. Pérez León for their assistance in the laboratory; A.
459 Lázaro, G. Escribano-Ávila, A. Payo-Payo and L. Cayuela for helpful comments on
460 mixed models. We also thank J. Flexas and C. Íñiguez for sharing their knowledge on
461 plant physiology, and J. Terrados for the logistic support. M.S.-M. was supported by a
462 Fundación “La Caixa” fellowship and the unemployment benefit of Spanish Ministry of
463 Labour, Migrations and Social Security. I.E.H. was supported by grant RYC-2014-
464 15147, co-funded by the Conselleria d'Innovació, Recerca i Turisme of the Balearic
465 Government (Pla de ciència, tecnologia, innovació i emprenedoria 2013-2017) and the
466 Spanish Ministry of Economy, Industry and Competitiveness.

467

468

469 **7 References**

470

471 Anton, A., Hendriks, I.E., Marbà, N., Krause-Jensen, D., Garcias-Bonet, N., Duarte,
472 C.M., 2018. Iron Deficiency in Seagrasses and Macroalgae in the Red Sea Is
473 Unrelated to Latitude and Physiological Performance. *Front. Mar. Sci.* 5, 1–14.
474 <https://doi.org/10.3389/fmars.2018.00074>

475 Apostolaki, E.T., Vizzini, S., Hendriks, I.E., Olsen, Y.S., 2014. Seagrass ecosystem

- 476 response to long-term high CO₂ in a Mediterranean volcanic vent. *Mar.*
477 *Environ. Res.* 99, 9–15. <https://doi.org/10.1016/j.marenvres.2014.05.008>
- 478 Bates, N.R., Moran, S.B., Hansell, D.A., Mathis, J.T., 2006. An increasing CO₂ sink in
479 the Arctic Ocean due to sea-ice loss. *Geophys. Res. Lett.* 33, 1–7.
480 <https://doi.org/10.1029/2006GL027028>
- 481 Beer, S., Björk, M., Beardall, J., 2014. *Photosynthesis in the marine environment.*
482 John Wiley & Sons.
- 483 Beer, S., Rehnberg, J., 1997. The acquisition of inorganic carbon by the seagrass
484 *Zostera marina*. *Aquat. Bot.* 56, 277–283.
- 485 Berge, J., Johnsen, G.H., Nilsen, F., Bjørn, G., Slagstad, D., 2005. Ocean temperature
486 oscillations enable reappearance of blue mussels *Mytilus edulis* in Svalbard
487 after a 1000 year absence. *Mar. Ecol. Prog. Ser.* 303, 167–175.
488 <https://doi.org/10.3354/meps303167>
- 489 Bonsell, C., Dunton, K.H., 2018. Long-term patterns of benthic irradiance and kelp
490 production in the central Beaufort sea reveal implications of warming for
491 Arctic inner shelves. *Prog. Oceanogr.* 162, 160–170.
492 <https://doi.org/10.1016/j.pocean.2018.02.016>
- 493 Bowes, G., 1985. Pathways of CO₂ fixation by aquatic organisms. Inorg. carbon
494 uptake by *Aquat. Photosynth. Org.* 187–210.
- 495 Bowes, G., Salvuci, M.E., 1989. Plasticity in the photosynthetic carbon metabolism
496 of submersed aquatic macrophytes. *Aquat Bot* 34, 233–266.
- 497 Coupel, P., Ruiz-Pino, D., Sicre, M.A., Chen, J., Lee, S.H., Schiffrine, N., Li, H.L.,
498 Gascard, J.C., 2015. The impact of freshening on phytoplankton production in
499 the Pacific Arctic Ocean. *Prog. Oceanogr.* 131, 113–125.
500 <https://doi.org/10.1016/j.pocean.2014.12.003>
- 501 Dickson, A.G., 1990. Standard potential of the reaction: AgCl (s)+ 1/2H₂ (g)= Ag
502 (s)+ HCl (aq), and the standard acidity constant of the ion HSO₄⁻ in
503 synthetic sea water from 273.15 to 318.15 K. *J. Chem. Thermodyn.* 22, 113–
504 127.
- 505 Dickson, A.G., Millero, F.J., 1987. A comparison of the equilibrium constants for the
506 dissociation of carbonic acid in seawater media. *Deep Sea Res. Part A.*
507 *Oceanogr. Res. Pap.* 34, 1733–1743.
- 508 Dickson, A.G., Sabine, C.L., Christian, J.R., 2007. *Guide to best practices for ocean*
509 *CO₂, PICES Special Publication.* North Pacific Marine Science Organization,
510 Sidney, British Columbia.
- 511 Duarte, C.M., Cebrián, J., 1996. The fate of marine autotrophic production. *Limnol.*
512 *Oceanogr.* 41, 1758–1766. <https://doi.org/10.4319/lo.1996.41.8.1758>
- 513 Engel, A., Piontek, J., Grossart, H.P., Riebesell, U., Schulz, K.G., Sperling, M., 2014.
514 Impact of CO₂ enrichment on organic matter dynamics during nutrient
515 induced coastal phytoplankton blooms. *J. Plankton Res.* 36, 641–657.
516 <https://doi.org/10.1093/plankt/fbt125>
- 517 Falkowski, P.G., Raven, J.A., 2013. *Aquatic photosynthesis, Freshwater Biology.*
518 Princeton University Press. <https://doi.org/10.1016/j.bmcl.2011.05.118>

- 519 Filbee-Dexter, K., Wernberg, T., Fredriksen, S., Norderhaug, K.M., Foldager, M.,
520 2019. Arctic kelp forests : Diversity , resilience and future. *Glob. Planet.*
521 *Change* 172, 1–14. <https://doi.org/10.1016/j.gloplacha.2018.09.005>
- 522 Florczyk, I., Latala, A., 1989. The phytobenthos of the Hornsund fiord, SW
523 Spitsbergen. *Polar Res.* 7, 29–41. [https://doi.org/10.1111/j.1751-](https://doi.org/10.1111/j.1751-8369.1989.tb00602.x)
524 [8369.1989.tb00602.x](https://doi.org/10.1111/j.1751-8369.1989.tb00602.x)
- 525 Fortes, M.D., Lüning, K., 1980. Growth rates of North Sea macroalgae in relation to
526 temperature, irradiance and photoperiod. *Helgoländer*
527 *Meeresuntersuchungen* 34, 15–29.
- 528 Fransson, A., Chierici, M., Nojiri, Y., 2009. New insights into the spatial variability of
529 the surface water carbon dioxide in varying sea ice conditions in the Arctic
530 Ocean. *Cont. Shelf Res.* 29, 1317–1328.
531 <https://doi.org/10.1016/j.csr.2009.03.008>
- 532 Fredriksen, S., Bartsch, I., Wiencke, C., 2014. New additions to the benthic marine
533 flora of Kongsfjorden, western Svalbard, and comparison between 1996/1998
534 and 2012/2013. *Bot. Mar.* 57, 203–216. [https://doi.org/10.1515/bot-2013-](https://doi.org/10.1515/bot-2013-0119)
535 [0119](https://doi.org/10.1515/bot-2013-0119)
- 536 Giordano, M., Beardall, J., Raven, J.A., 2005. CO₂ concentrating mechanisms in algae:
537 mechanisms, environmental modulation, and evolution. *Annu. Rev. Plant Biol.*
538 56, 99–131. <https://doi.org/10.1146/annurev.arplant.56.032604.144052>
- 539 Giordano, M., Maberly, S.C., 1989. Distribution of carbonic anhydrase in British
540 marine macroalgae. *Oecologia* 81, 534–539.
541 <https://doi.org/10.1007/BF00378965>
- 542 Gordillo, F.J.L., Aguilera, J., Jiménez, C., 2006. The response of nutrient assimilation
543 and biochemical composition of Arctic seaweeds to a nutrient input in
544 summer. *J. Exp. Bot.* 57, 2661–2671. <https://doi.org/10.1093/jxb/erl029>
- 545 Hanelt, D., 1996. Photoinhibition of photosynthesis in marine macroalgae. *Sci. Mar.*
546 60, 243–248.
- 547 Hansen, J.R., Haugen, I., 1989. Some observations of intertidal communities on
548 Spitsbergen (79°N), Norwegian Arctic. *Polar Res.* 7, 23–27.
549 <https://doi.org/10.1111/j.1751-8369.1989.tb00601.x>
- 550 Harrison, W.G., Platt, T., 1986. Photosynthesis-irradiance relationship in polar and
551 temperate phytoplankton populations. *Polar Biol.* 5, 153–164.
- 552 Hein, M., Sand-Jensen, K., 1997. CO₂ increases oceanic primary production. *Nature*
553 388, 526–527.
- 554 Hendriks, I.E., Duarte, C.M., Marbà, N., Krause-Jensen, D., 2017. pH gradients in the
555 diffusive boundary layer of subarctic macrophytes. *Polar Biol.* 1–6.
556 <https://doi.org/10.1007/s00300-017-2143-y>
- 557 Holbrook, G.P., Beer, S., Spencer, W.E., Reiskind, J.B., Davis, J.S., Bowes, G., 1987.
558 Photosynthesis in marine macroalgae: evidence for carbon limitation. *Can. J.*
559 *Bot.* 66, 577–582.
- 560 Holding, J.M., Duarte, C.M., Sanz-Martín, M., Mesa, E., Arrieta, J.M., Chierici, M.,
561 Hendriks, I.E., García-Corral, L.S., Regaudie-De-Gioux, A., Delgado-Huertas, A.,

- 562 Reigstad, M., Wassmann, P.F., Agustí, S., 2015. Temperature dependence of
563 CO₂-enhanced primary production in the European Arctic Ocean. *Nat. Clim.*
564 *Chang.* 8–11. <https://doi.org/10.1038/nclimate2768>
- 565 Hoppe, C.J.M., Holtz, L.M., Trimborn, S., Rost, B., 2015. Ocean acidification decreases
566 the light-use efficiency in an Antarctic diatom under dynamic but not constant
567 light. *New Phytol.* 207, 159–171. <https://doi.org/10.1111/nph.13334>
- 568 Hoppe, C.J.M., Wolf, K.K.E., Schuback, N., Tortell, P.D., Rost, B., 2018. Compensation
569 of ocean acidification effects in Arctic phytoplankton assemblages. *Nat. Clim.*
570 *Chang.* 8, 529–533. <https://doi.org/10.1038/s41558-018-0142-9>
- 571 Hoppe, J.C.M., Schuback, N., Semeniuk, D.M., Maldonado, M.T., Rost, B., 2017.
572 Functional Redundancy Facilitates Resilience of Subarctic Phytoplankton
573 Assemblages toward Ocean Acidification and High High Irradiance. *Front. Mar.*
574 *Sci.* 4, 1–14. <https://doi.org/10.3389/fmars.2017.00229>
- 575 Hurd, C.L., Hepburn, C.D., Currie, K.I., Raven, J.A., Hunter, K.A., 2009. Testing the
576 effects of ocean acidification on algal metabolism: Considerations for
577 experimental designs. *J. Phycol.* 45, 1236–1251.
578 <https://doi.org/10.1111/j.1529-8817.2009.00768.x>
- 579 Iñiguez, C., Carmona, R., Lorenzo, M.R., Niell, F.X., Wiencke, C., Gordillo, F.J.L., 2016.
580 Increased CO₂ modifies the carbon balance and the photosynthetic yield of
581 two common Arctic brown seaweeds: *Desmarestia aculeata* and *Alaria*
582 *esculenta*. *Polar Biol.* 39, 1979–1991. <https://doi.org/10.1007/s00300-015-1724-x>
- 584 Iñiguez, C., Heinrich, S., Harms, L., Gordillo, F.J.L., 2017. Increased temperature and
585 CO₂ alleviate photoinhibition in *Desmarestia anceps*: from transcriptomics to
586 carbon utilization. *J. Exp. Bot.* <https://doi.org/10.1093/jxb/erx164>
- 587 IPCC Panel, 2014. *Climate Change 2014: Synthesis Report*, Contributi. ed. Geneva,
588 Switzerland.
- 589 Johnston, A.M., Raven, J.A., 1986. The utilization of bicarbonate ions by the
590 macroalga *Ascophyllum nodosum* (L.) Le Jolis. *Plant. Cell Environ.* 9, 175–184.
- 591 Kjesbu, O.S., Bogstad, B., Devine, J.A., Gjørseter, H., Howell, D., Ingvaldsen, R.B.,
592 Nash, R.D.M., Skjæraasen, J.E., 2014. Synergies between climate and
593 management for Atlantic cod fisheries at high latitudes. *Proc. Natl. Acad. Sci.*
594 111, 3478–3483. <https://doi.org/10.1073/pnas.1316342111>
- 595 Koch, M., Bowes, G., Ross, C., Zhang, X.H., 2013. Climate change and ocean
596 acidification effects on seagrasses and marine macroalgae. *Glob. Chang. Biol.*
597 19, 103–132. <https://doi.org/10.1111/j.1365-2486.2012.02791.x>
- 598 Krause-Jensen, D., Duarte, C.M., 2014. Expansion of vegetated coastal ecosystems in
599 the future Arctic. *Front. Mar. Sci.* 1, 1–10.
600 <https://doi.org/10.3389/fmars.2014.00077>
- 601 Krause-Jensen, D., Marbà, N., Olesen, B., Sej, M.K., Christensen, P.B., Rodrigues, J.,
602 Renaud, P.E., Balsby, T.J.S., Rysgaard, S., 2012. Seasonal sea ice cover as
603 principal driver of spatial and temporal variation in depth extension and
604 annual production of kelp in Greenland. *Glob. Chang. Biol.* 18, 2981–2994.
605 <https://doi.org/10.1111/j.1365-2486.2012.02765.x>

- 606 Krause-Jensen, D., Marbà, N., Sanz-Martín, M., Hendriks, I.E., Thyrring, J.,
607 Carstensen, J., Sejr, M.K., Duarte, C.M., 2016. Long photoperiods sustain high
608 pH in Arctic kelp forests. *Sci. Adv.* 2, 1–8.
609 <https://doi.org/10.1126/sciadv.1501938>
- 610 Madsen, T. V., Sand-Jensen, K., 1991. Photosynthetic carbon assimilation in aquatic
611 macrophytes. *Aquat. Bot.* 41.
- 612 Marbà, N., Krause-Jensen, D., Olesen, B., Christensen, P.B., Merzouk, A., Rodrigues,
613 J., Wegeberg, S., Wilce, R.T., 2017. Climate change stimulates the growth of the
614 intertidal macroalgae *Ascophyllum nodosum* near the northern distribution
615 limit. *Ambio* 46, 119–131. <https://doi.org/10.1007/s13280-016-0873-7>
- 616 McLaughlin, F.A., Carmack, E.C., 2010. Deepening of the nutricline and chlorophyll
617 maximum in the Canada Basin interior, 2003–2009. *Geophys. Res. Lett.* 37, 1–
618 5. <https://doi.org/10.1029/2010GL045459>
- 619 McMinn, A., Martin, A., Ryan, K., 2010. Phytoplankton and sea ice algal biomass and
620 physiology during the transition between winter and spring (McMurdo Sound,
621 Antarctica). *Polar Biol.* 33, 1547–1556. <https://doi.org/10.1007/s00300-010-0844-6>
- 623 Mehrbach, C., Culberson, C.H., Hawley, J.E., Pytkowicz, R.M., 1973. Measurement of
624 the apparent dissociation constants of carbonic acid in seawater at
625 atmospheric pressure. *Limnol. Oceanogr.* 18, 897–907.
- 626 Meire, L., Søgaard, D.H., Mortensen, J., Meysman, F.J.R., Soetaert, K., Arendt, K.E.,
627 Juul-Pedersen, T., Blicher, M.E., Rysgaard, S., 2015. Glacial meltwater and
628 primary production are drivers of strong CO₂ uptake in fjord and coastal
629 waters adjacent to the Greenland Ice Sheet. *Biogeosciences* 12, 2347–2363.
630 <https://doi.org/10.5194/bg-12-2347-2015>
- 631 Mercado, J.M., de los Santos, C.B., Lucas Pérez-Llorens, J., Vergara, J.J., 2009. Carbon
632 isotopic fractionation in macroalgae from Cádiz Bay (Southern Spain):
633 Comparison with other bio-geographic regions. *Estuar. Coast. Shelf Sci.* 85,
634 449–458. <https://doi.org/10.1016/j.ecss.2009.09.005>
- 635 Mercado, J.M., Gordillo, F., 2011. Inorganic carbon acquisition in algal communities:
636 are the laboratory data relevant to the natural ecosystems? *Photosynth. Res.*
637 109, 257–67. <https://doi.org/10.1007/s11120-011-9646-0>
- 638 Olesen, B., Krause-Jensen, D., Marbà, N., Christensen, P.B., 2015. Eelgrass *Zostera*
639 *marina* in subarctic Greenland: Dense meadows with slow biomass turnover
640 in cold waters. *Mar. Ecol. Prog. Ser.* 518, 107–121.
641 <https://doi.org/10.3354/meps11087>
- 642 Pierrot, D., Lewis, E.R., Wallace, D.W.R., 2006. MS excel program developed for CO₂
643 system calculations. Carbon dioxide information analysis center, Oak Ridge
644 National Laboratory. US Department of Energy, Oak Ridge, Tennessee.
- 645 Platt, T., Harrison, W.G., Irwin, B., Horne, E.P., Gallegos, C.L., 1982. Photosynthesis
646 and photoadaptation of marine phytoplankton in the Arctic. *Deep Sea Res.* 29,
647 1159–1170.
- 648 Post, E., Bhatt, U.S., Bitz, C.M., Brodie, J.F., Fulton, T.L., Hebblewhite, M., Kerby, J.,
649 Kutz, S.J., Stirling, I., Walker, D.A., 2013. Ecological consequences of sea-ice

650 decline. *Science* (80-.). 341, 519–525.

651 R Core Team, 2014. R: A language and environment for statistical computing. R
652 Foundation for Statistical Computing, Vienna, Austria. 2013.

653 Ralph, P.J., Gademann, R., 2005. Rapid light curves: A powerful tool to assess
654 photosynthetic activity. *Aquat. Bot.* 82, 222–237.
655 <https://doi.org/10.1016/j.aquabot.2005.02.006>

656 Raven, J.A., Johnston, A.M., Kübler, J.E., Korb, R., McInroy, S.G., Handley, L.L.,
657 Scrimgeour, C.M., Walker, D.I., 2002a. Mechanistic interpretation of carbon
658 isotope discrimination by marine macroalgae and seagrasses. *Funct. Plant
659 Biol.* 29, 335–378. <https://doi.org/10.1071/PP01201>

660 Raven, J.A., Johnston, A.M., Kübler, J.E., Korb, R., McInroy, S.G., Handley, L.L.,
661 Scrimgeour, C.M., Walker, D.I., Beardall, J., Clayton, M.N., Vanderklift, M.,
662 Fredriksen, S., Dunton, K.H., 2002b. Seaweeds in cold seas: Evolution and
663 carbon acquisition. *Ann. Bot.* 90, 525–536.
664 <https://doi.org/10.1093/aob/mcf171>

665 Raven, J.A., Osmond, C.B., 1992. Inorganic C acquisition processes and their
666 ecological significance in inter- and sub-tidal macroalgae of North Carolina.
667 *Funct. Ecol.* 6, 41–47.

668 Rysgaard, S., Bendtsen, J., Pedersen, L.T., Ramløv, H., Glud, R.N., 2009. Increased
669 CO₂ uptake due to sea ice growth and decay in the Nordic Seas. *J. Geophys.
670 Res.* 114, C09011. <https://doi.org/10.1029/2008JC005088>

671 Sand-Jensen, K., Gordon, D.M., 1984. Differential ability of marine and freshwater
672 macrophytes to utilize HCO₃⁻ and CO₂. *Mar. Biol.* 80, 247–253.
673 <https://doi.org/10.1038/470444a>

674 Silva, J., Santos, R., Calleja, M.L., Duarte, C.M., 2005. Submerged versus air-exposed
675 intertidal macrophyte productivity: from physiological to community-level
676 assessments. *J. Exp. Mar. Bio. Ecol.* 317, 87–95.
677 <https://doi.org/10.1016/j.jembe.2004.11.010>

678 Sorte, C.J.B., Williams, S.L., Carlton, J.T., 2010. Marine range shifts and species
679 introductions: Comparative spread rates and community impacts. *Glob. Ecol.
680 Biogeogr.* 19, 303–316. <https://doi.org/10.1111/j.1466-8238.2009.00519.x>

681 Strömgren, T., 1978. The effect of photoperiod on the length growth of five species
682 of intertidal fucales. *Sarsia* 63, 155–157.

683 Surif, M.B., Raven, J.A., 1989. Exogenous inorganic carbon sources for
684 photosynthesis in seawater by members of the Fucales and the Laminariales
685 (Phaeophyta): ecological and taxonomic implications. *Oecologia* 78, 97–105.
686 <https://doi.org/10.1007/BF00377203>

687 Takahashi, T., Sutherland, S.C., Wanninkhof, R., Sweeney, C., Feely, R.A., Chipman,
688 D.W., Hales, B., Friederich, G., Chavez, F., Sabine, C., Watson, A., Bakker, D.C.E.,
689 Schuster, U., Metzl, N., Yoshikawa-Inoue, H., Ishii, M., Midorikawa, T., Nojiri, Y.,
690 Körtzinger, A., Steinhoff, T., Hoppema, M., Olafsson, J., Arnarson, T.S., Tilbrook,
691 B., Johannessen, T., Olsen, A., Bellerby, R., Wong, C.S., Delille, B., Bates, N.R., de
692 Baar, H.J.W., 2009. Climatological mean and decadal change in surface ocean
693 pCO₂, and net sea-air CO₂ flux over the global oceans. *Deep. Res. Part II Top.*

694 Stud. Oceanogr. 56, 554–577. <https://doi.org/10.1016/j.dsr2.2008.12.009>

695 Traiger, S.B., Konar, B., 2018. Journal of Experimental Marine Biology and Ecology
696 Mature and developing kelp bed community composition in a glacial estuary.
697 J. Exp. Mar. Bio. Ecol. 501, 26–35.
698 <https://doi.org/10.1016/j.jembe.2017.12.016>

699 Velez Ramirez, A.I., Ieperen, W. van, Vreugdenhill, D., Millenaar, F.F., 2011. Plants
700 under continuous light. Trends Plant Sci. 16, 310–318. <https://doi.org/Doi>
701 [10.1016/J.Tplants.2011.02.003](https://doi.org/10.1016/J.Tplants.2011.02.003)

702 Wang, M., Overland, J.E., 2009. A sea ice free summer Arctic within 30 years?
703 Geophys. Res. Lett. 36, 2–6. <https://doi.org/10.1029/2009GL037820>

704 Weslawski, J.M., Wiktor, J., Kotwicki, L., 2010. Increase in biodiversity in the arctic
705 rocky littoral, Sorkappland, Svalbard, after 20 years of climate warming. Mar.
706 Biodivers. 40, 123–130. <https://doi.org/10.1007/s12526-010-0038-z>

707 Wilce, R., Dunton, K.H., 2014. The boulder Patch (North Alaska, Beaufort Sea) and
708 its benthic algal flora. Arctic 67, 43–56. <https://doi.org/10.14430/arctic4360>

709 Wulff, A., Iken, K., Quartino, M.L., Al-Handal, A., Wiencke, C., Clayton, M.N., 2009.
710 Biodiversity, biogeography and zonation of marine benthic micro- and
711 macroalgae in the Arctic and Antarctic. Bot. Mar. 52, 491–507.
712 <https://doi.org/10.1515/BOT.2009.072>

713 Yun, M.S., Whitley, T.E., Stockwell, D., Son, S.H., Lee, J.H., Park, J.-W., Lee, S.H.,
714 2016. Primary production in the Chukchi Sea with potential effects of
715 freshwater content. Biogeosciences 13, 737–749.
716 <https://doi.org/10.5194/bg-13-737-2016>

717 Zeebe, R.E., 2012. History of seawater carbonate chemistry, atmospheric CO₂, and
718 ocean acidification. Annu. Rev. Earth Planet. Sci. 40, 141–165.
719 <https://doi.org/10.1146/annurev-earth-042711-105521>

720

721

722

723

724

725

726

727

728

729

730

731

732

733

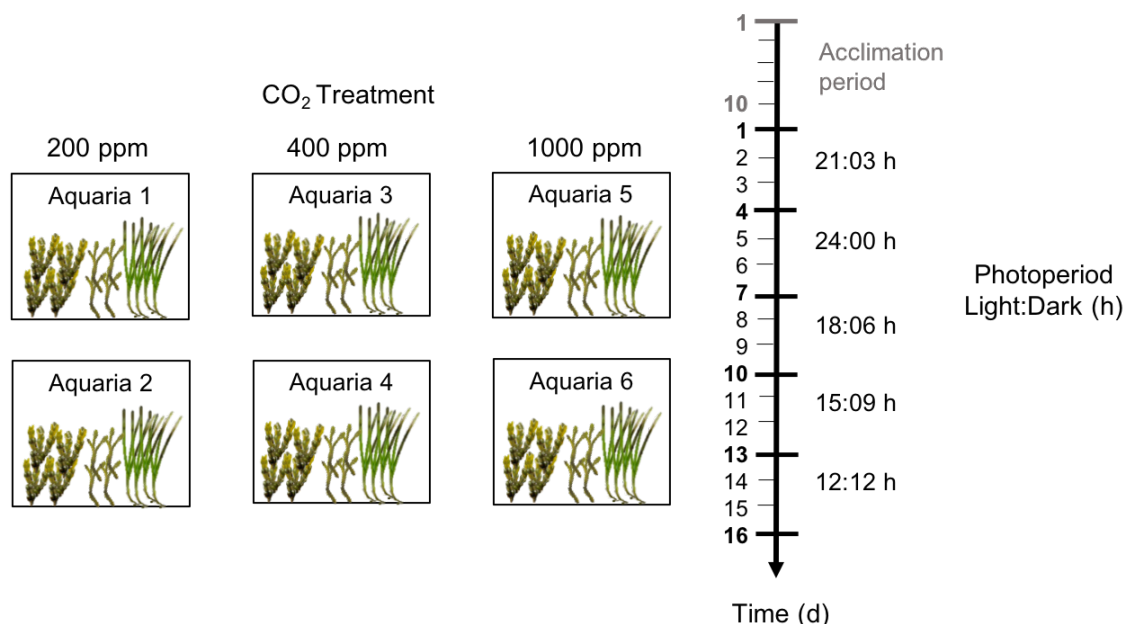
734

735

736

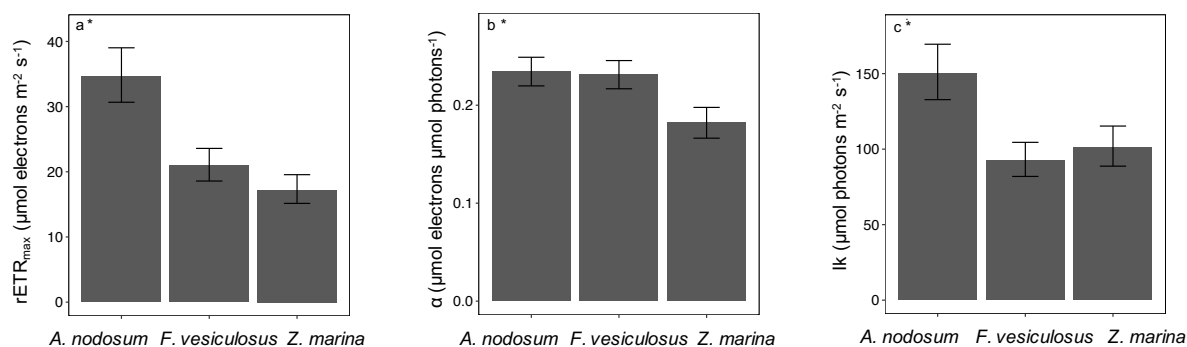
737
738

8 Figures and tables



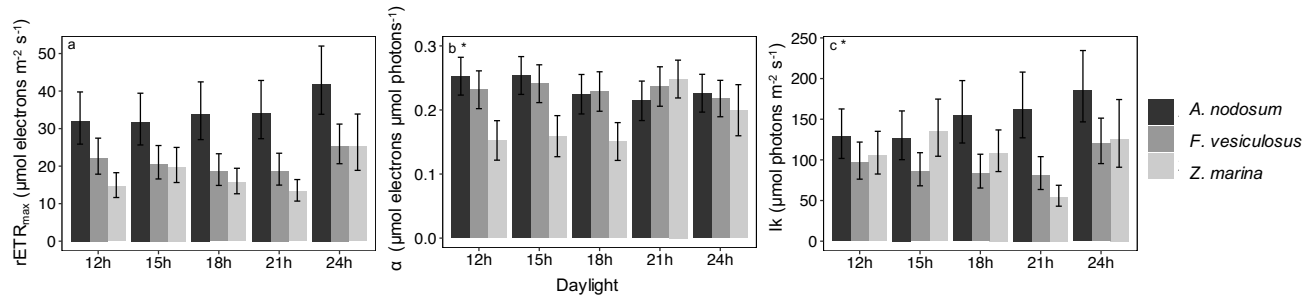
739
740
741
742
743
744
745

Figure 1: Experimental set-up, analysed with a split-plot model, where specimens of *Fucus vesiculosus*, *Ascophyllum nodosum* and *Zostera marina* were placed into replicated aquaria. After the acclimation period, the CO₂ treatments were applied throughout the experiment and light treatments (i.e. photoperiods) were changed every three days.



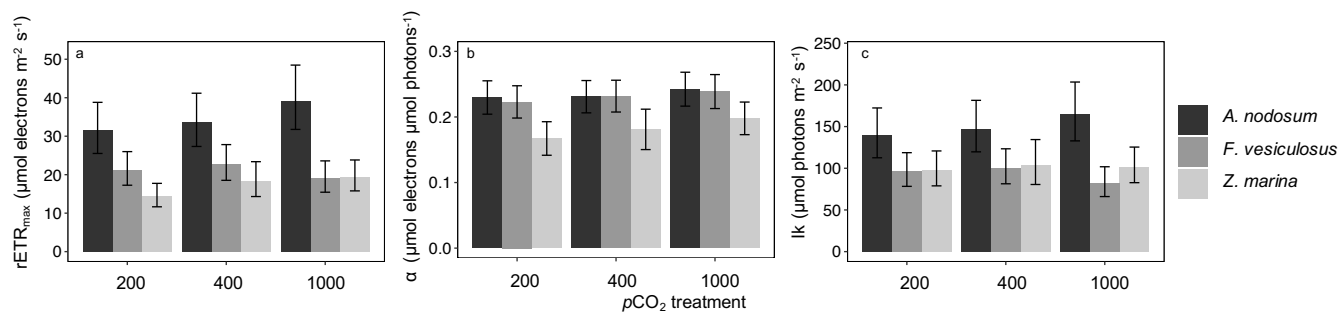
746
747
748
749
750
751
752
753
754

Figure 2: Estimated means of $rETR_{max}$, and saturating irradiance, I_k (a, b, c, respectively) as calculated for different species (*Ascophyllum nodosum*, *Fucus vesiculosus* and *Zostera marina*) as the average of the levels of daylight and the pCO_2 treatments. Significance is indicated with an asterisk ($p < 0.05$). Error bars mark standard errors of the means.



755
756
757
758
759
760
761
762
763
764
765
766

Figure 3: Estimated means of $rETR_{max}$, (a) α (b) and saturating irradiance, I_k (c) for different combinations of photoperiod and species (*Ascophyllum nodosum*, *Fucus vesiculosus* and *Zostera marina*), i.e. $s_k \times p_j$ in the mixed model. Significance of the interaction is indicated with an asterisk ($p < 0.05$). Error bars mark standard errors of the means.



767
768
769
770
771
772
773
774
775
776
777
778

Figure 4: Estimated means of $rETR_{max}$ (a), α (b) and saturating irradiance, I_k (c) for different combinations of pCO_2 treatments and species (*Ascophyllum nodosum* in black, *Fucus vesiculosus* in dark grey and *Zostera marina* in light grey), i.e. $s_k \times c_i$ in the mixed model. Significance of the interaction is indicated with an asterisk ($p < 0.05$) (none of them). Error bars mark standard errors of the means.

779 **Table 1:** Statistical tests of the fixed effects for the three photosynthetic responses.
 780 Denominator degrees of freedom was calculated with Satterthwaite's approximation.
 781 Asterisk on the effect column indicates the interaction between factors while asterisk on
 782 the p-value column indicate the significance ($p < 0.05$)
 783

Parameter	Effect	Numerator Df	Denominator Df	F-value	p-value
rETR _{max}	CO ₂ treatment	2	9.0	1.4	0.30
rETR _{max}	Photoperiod	4	14.6	4.6	0.01 *
rETR _{max}	Photoperiod*CO ₂ treatment	8	14.2	0.7	0.72
rETR _{max}	Species	2	8.6	34.9	7.7E-05 *
rETR _{max}	CO ₂ treatment*Species	4	8.4	1.3	0.34
rETR _{max}	Photoperiod*Species	8	87.5	1.3	0.27
rETR _{max}	Photoperiod*CO ₂ Treatment*Species	16	85.9	0.6	0.88
α	CO ₂ treatment	2	9.9	1.8	0.22
α	Photoperiod	4	33.4	1.7	0.17
α	Photoperiod*CO ₂ treatment	8	32.7	0.7	0.68
α	Species	2	9.8	14.1	1.3E-03 *
α	CO ₂ treatment*Species	4	9.7	0.2	0.95
α	Photoperiod*Species	8	32.8	3.8	2.9E-03 *
α	Photoperiod*CO ₂ Treatment*Species	16	32.1	1.5	0.14
lk	CO ₂ treatment	2	3.0	0.1	0.90
lk	Photoperiod	4	13.0	4.8	0.01 *
lk	Photoperiod*CO ₂ treatment	8	12.6	1.4	0.28
lk	Species	2	23.6	23.9	2.1E-06 *
lk	CO ₂ treatment*Species	4	23.1	1.0	0.41
lk	Photoperiod*Species	8	91.4	3.8	7.3E-04 *
lk	Photoperiod*CO ₂ Treatment*Species	16	90.2	1.1	0.38

784